BBAMEM 74583

The lyotropic liquid crystal properties of *n*-octyl 1-*O*-β-D-glucopyranoside and related *n*-alkyl pyranosides

Yong Je Chung and George A. Jeffrey

Department of Crystallography, University of Pittsburgh, Pittsburgh, PA (U.S.A.)

X-ray diffraction patterns have been obtained for the lyotropic phases of *n*-octyl 1-*O*-β-D-glucopyranoside and the related *n*-heptyl, *n*-nonyl and *n*-decyl compounds with water. The octyl compound exhibits all three liquid crystal phases and forms a micellar solution with increasing solvation, when the crystal come into contact with water at room temperature. The X-ray diffraction patterns show a one-dimensional lamellar phase with $\langle d_x \rangle = 28.4$ Å, a three-dimensional face-centered cubic phase with $\langle a \rangle = 51.2$ Å, and a two-dimensional hexagonal phase with $\langle a \rangle = \langle b \rangle = 36.7$ Å. The micellar solution has a distribution pattern with a maximum at $\langle d_x \rangle = 33.8$ Å. Crystals of the heptyl, nonyl and decyl derivatives form only the lamellar phases and the micellar solution on contact with water at room temperature.

β-OG (*n*-octyl 1-*O*-β-D-glucopyranoside) is a non-ionic surfactant used for solubilizing and crystallizing membrane proteins [1,2]. It was the first of a series of carbohydrates to be recognized as useful for this purpose [3–7]. It has also been shown to promote the rate of crystal growth of some soluble proteins [8]. The crystalline solid displays both thermotropic and lyotropic liquid crystal phases. The former was observed on heating to 68.2 ° C [9], the latter on contact with water at room temperature. The lyotropic behavior follows the classical pattern established for the ionic detergents, such as the soaps [10]. As the water penetrates a polycrystalline sample, dissolution takes place forming a concentration gradient. The lamellar, cubic, hexagonal liquid crystal phases and the micellar solution are concentrically developed as shown schematically in Fig. 1, and can be identified by their characteristic optical properties under a polarizing microscope. In this paper we report the corresponding X-ray diffraction pattern recorded on an area detector with short exposure times of one or two minutes. The structural information these patterns provide concerning the organization of the molecular clusters in the liquid crystal phases is interpreted in terms of the models used to describe the lamellar, cubic and hexagonal phases of soaps [10].

The *n*-heptyl, *n*-nonyl and *n*-decyl β-glucopyranosides which are also used as membrane surfactants, have similar, but less elegant lyotropic behavior with water at room temperature displaying only the lamellar phase and the micellar solution.

Material and Methods

The samples of *n*-heptyl to *n*-decyl β-D-glucopyranoside (98% purity) were obtained from Sigma Chemical Co., and used without recrystallization. Optical observation was made with a Zeiss polarizing microscope by placing a cover-slip over a few crystals and allowing water to diffuse inward from the edge at room temperature. Dissolution of the β-OG took place over about 15 minutes during which all three liquid crystal phases were observed, as shown schematically in Fig. 1. For one series of X-ray diffraction experiments the crystalline powder was placed in a capillary 1.0 mm diameter and water was added at room temperature. In a second series, the crystalline powder was melted and allowed to solidify before the supernatant water was added. As the water penetrated the solid, the three liquid crystal phases were formed and clearly delineated under the polarizing microscope, as shown schematically in Fig. 2. The melted solid gave the clearer definition and was used for the diffraction measurements. The phases developed in the capillary over a period of about 2 hours and were stable for several hours.

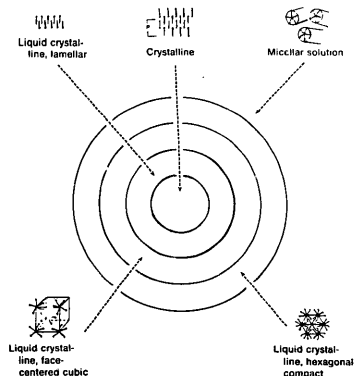This type of sample preparation was recently applied to construct a temperature-composition-mesomorph di-

Fig. 1. Diagrammatic representation of the lyotropic liquid crystal phases formed by the concentration gradient of β-OG and water.
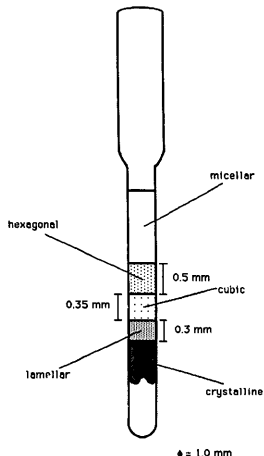

Fig. 2. Schematic of the liquid crystal phase formation in the capillary sample used for X-ray diffraction.

agram using time-resolved X-ray diffraction techniques [11]. The results agree well with those obtained by conventional methods.

X-ray patterns were recorded on a Nicolet X100 area detector with a Rigaku rotating anode X-ray tube (CuK$_\alpha$; 55 kV, 200 mA, collimator diameter: 0.25 mm) by moving the different liquid crystal phases successively into the X-ray beam. The exposure time was 120 seconds. The sample to detector distance was 210 nm.

The intensity versus 2θ shown in Figs. 3–6 were obtained by counting the phonons recorded in each adjacent pixel on the area detector.

Since no method was available for measuring the concentration gradient of the lyotropic phases formed continuously in the capillary, the X-ray beam was directed at the mid-point of each segment and the mean concentration for each phase was measured by means of separate experiments. Concentrations were measured by weighing capillaries as the phases were formed by evaporation of the water. The mean values used were the average value for each phase. The phases were identified by their characteristic birefringence, or lack of it as in the cubic case. The mean concentrations for the lamellar, cubic and hexagonal phases of β-OG are 85, 75 and 65% by weight, respectively, and varied by ±5% over each phase.

The dimensions of the surfactant molecular clusters in the liquid crystal phases were calculated from the mean X-ray d-spacing $\langle d_x \rangle$ using Luzzati's equations [12], defined in the Appendix. The partial specific volume of the surfactant, v_s, was assumed to be 0.8 cm$^2 \cdot$ g^{-1} taken from the density and the known crystal structure of the octyl α-glucopyranoside hemi and monohydrates [13].

The greatest uncertainty is in the mean concentration values. These affect the values of d_1 proportionally, but less so for the hexagonal and cubic phases, where the dependency on concentration is as the square and cube roots, respectively.

Results and Discussion

The crystalline phase

No crystal structures of the heptyl to decyl β-glucopyranosides have been determined due to the difficulty of obtaining crystals large enough for single crystal X-ray structure analysis. Crystal structures of the less soluble octyl and decyl α-D-glucopyranosides have been reported [13,14].

The powder diffraction pattern of the β-OG used in these experiments was not consistent with the periodicities of 29.4 Å and 4.88 Å measured from a single crystal electron diffraction photograph [9].

All the crystal structures of the long chain 1-O and 1-S alkyl pyranosides hitherto determined have head-to-head bilayer molecular packing with interdigitating
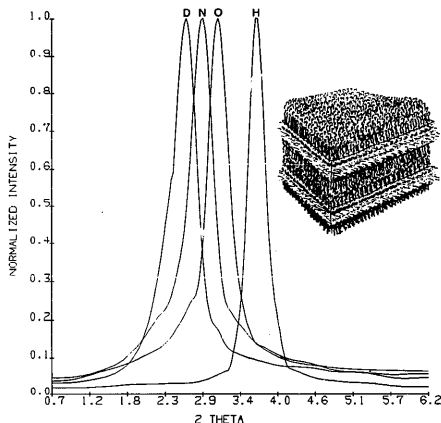
302

Fig. 3. One-dimensional X-ray intensity distribution for the lamellar liquid crystal phases of heptyl (H), octyl (O), nonyl (N) and decyl (D) β-glucopyranosides.

alkyl chains irrespective of whether they are the α or β epimers [15,16]. The pyranose headgroups are strongly hydrogen-bonded in cooperative systems which are characteristic of the pyranose and alkyl pyranoside crystal structures * [17]. In these crystal structures the ratio of the width of the bilayer and the molecular length, i.e., from furthest extended hydroxyl hydrogen on the sugar moiety to the furthest extended methyl hydrogen on the alkyl moiety, depends on the angle of inclination of the alkyl chains to the median plane of the bilayer.

The lamellar phase

All four alkyl β-glucopyranosides formed lamellar liquid crystal phases which are identified by their anisotropic optical properties under the polarizing microscope. The diffraction patterns consisted of a single well-defined intense ring corresponding to a relatively

narrow one-dimensional distribution of periodicities, as shown in Fig. 3.

No higher order reflections were observed. This could be due to 'stacking disorder' [21] or 'dynamic disorder' caused by concentration gradient along the capillary. The mean d-spacings, $\langle d_x \rangle$, and the width at half-height, $\Delta\theta^0$, are given in Table I. The mean bilayer thickness of β-OG, $\langle d_1 \rangle$, for the mean concentration of 85% surfactant calculated by the Luzzati method (see Appendix), 23.3 Å, is 1.7-times the length of the fully extended molecules, extrapolated from models and the dimensions provided by the crystal structure of the α epimer. Similar ratios between bilayer thicknesses and molecular lengths are found for the lamellar type thermotropic

TABLE I

The mean observed spacings, $\langle d_x \rangle$, and the width at half-height intensity, $\Delta\theta^0$, for the lamellar phases of the heptyl to decyl β-glucopyranosides

Surfactants	$\langle d_x \rangle$ (Å)	$\Delta\theta^0$ at half height
Heptyl	23.7	0.27
Octyl [a]	28.4	0.34
Nonyl	30.6	0.38
Decyl	33.1	0.41

[a] Mean bilayer thickness, $\langle d_1 \rangle$, for mean concentration of 85% surfactant: 23.3 Å.

---

* This is not true for all the alditol alkylamides (straight-chain sugar derivatives). In that class of surfactants, which includes the MEGA-n series, two types of molecular packing are obtained in the crystalline state, head-to-head bilayers with intercalating even numbered carbon alkyl chains and head-to-tail monolayers with non-intercalating odd numbered carbon alkyl chains [18,19]. In the related N-alkyl gluconamides, both even and odd alkyl chain members have the head-to-tail monolayer structure with non-intercalating alkyl chains [20].

smectic-A phases of the alkyl glucosides [22]. This is interpreted as evidence for a structure with a hydrogen bonded carbohydrate core with more flexible and partially folded alkyl chains.
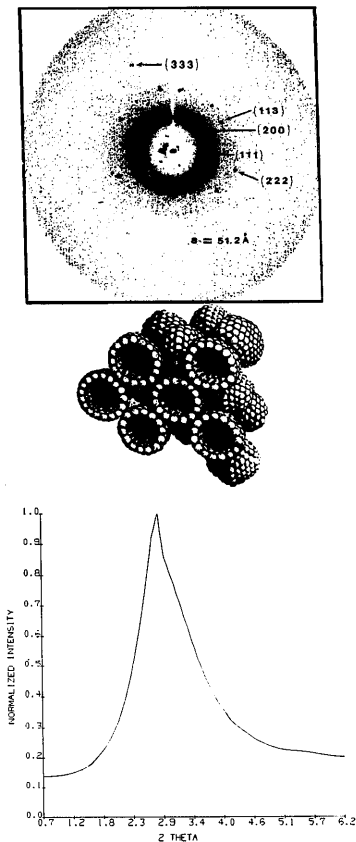

Fig. 4. X-ray diffraction pattern of the cubic lyotropic phase of β-OG showing both discrete spectra of a three-dimensional lattice and the diffuse ring of a one-dimensional distribution.
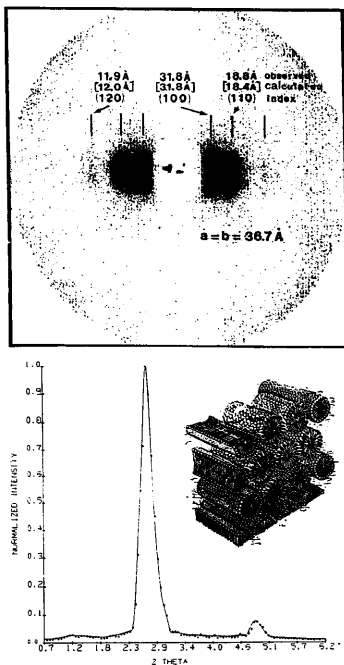

Fig. 5. X-ray diffraction pattern and intensity distribution for the hexagonal lyotropic phase of β-OG.

In this experiment, the systematic comparison among bilayer thickness of four related n-alkyl pyranosides is not appropriate, because a concentration measurement error can cause greater deviation than a difference in chain length. The difference in $\langle d_x \rangle$ between heptyl and nonyl is 6.9 Å, versus 4.7 Å between octyl and decyl. Molecules with odd and even numbered alkyl chains pack differently in their crystal structures, and the same effect might be expected in the lamellar bilayers.

The cubic phase

This highly viscous phase is observed, at room temperature, only with β-OG. It is identified under the polarizing microscope by the absence of birefringence

TABLE II

The d spacings of discrete spectra of the cubic phase in the β-OG/water system

Index	d spacing (Å)	
	calculated	observed
1 1 1	29.5	29.5 [a]
2 0 0	25.6	25.4
3 1 1	15.4	15.9
2 2 2	14.8	14.8
3 3 3	9.9	9.8

[a] Calibrated to d_{calc}. Diffuse ring: $d_{max} = 31.2$ Å, half-height width ($\Delta\theta$) = 1.03°.

occurring in a band between the lamellar and hexagonal phases. The diffraction pattern shown in Fig. 4 consists of discrete spectra and a diffuse ring. The discrete spectra are relatively sharp indicating crystalline domains exceeding ≈ 1000 Å in cross-section. Their distributions vary with sample preparation. Within the X-ray beam of diameter 0.25 mm and sample thickness of 1.0 mm, there are of the order of 20 domains in the correct orientation for Bragg diffraction with any one stationary sample. The sharp diffraction spectra can be indexed on a face-centered cubic lattice, Fm3m, with $\bar{a} = 51.2$ Å as shown in Table II. With an mean surfactant concentration of 75%, the corresponding radius of

the molecular clusters is ≈ 18 Å which is in agreement with the close contact distance of spheres or cylinders in a face-centered cubic lattice, since $\bar{a}/\sqrt{2} = 36.2$ Å. This indicates that some surfactant-surfactant contacts between clusters are necessary, thus resulting in highly viscous lyotropic liquid crystal phase. The absence of the face diagonal (220) reflection could be due to some preferred orientation in the capillary specimen or a consequence of the internal structure of the molecular cluster, which is presently unknown.

The diffuse ring has smaller spacing ($\langle d_x \rangle = 31.2$ Å) than in the micellar solution, but the one-dimensional distribution of periodicities is similar, as shown in Fig. 4. We interpret this as arising from the viscous micellar solution in which the cubic crystallite domains are suspended, since it shows no birefringence.

The hexagonal phase

Only β-OG exhibits a hexagonal phase at room temperature. The diffraction pattern consists of three arcs, corresponding to a two-dimensional distribution, as shown in Fig. 5. The intensities are very strong, strong, and weak, and can be indexed as (100), (110), (120) in the hexagonal plane group, P6, with $\bar{a} = \bar{b} = 36.7$ Å. With the mean surfactant concentration of 65%, the diameter of the cylindrical clusters is ≈ 30 Å which is approximately twice the molecular length, l_m, in agreement with the accepted model for the structure of a hexagonal lyotropic liquid crystal phase.
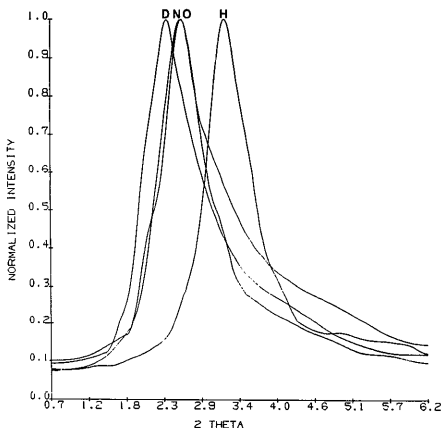

Fig. 6. One-dimensional intensity distribution for the micellar solutions of heptyl (H), octyl (O), nonyl (N) and decyl (D) β-glucopyranosides.
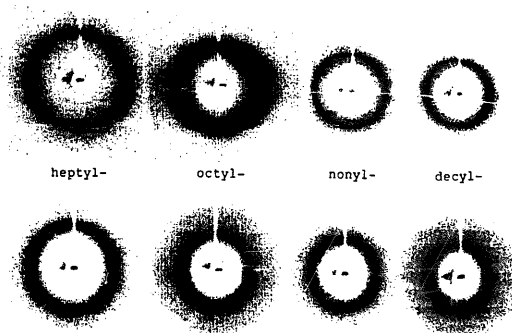
Fig. 7. Comparison of lamellar (up) and micellar (down) X-ray diffraction patterns.

The micellar solutions

All four alkyl β-glucopyranosides form micellar solutions and give diffraction patterns for one-dimensional distributions which are broader than those of the lamellar phase as shown in Figs. 6 and 7.

The mean $\langle d_x \rangle$ values and the width of $\langle d_x \rangle$ at half height intensity are given in Table III. They correspond to greater than twice the length of the extended molecule. The d_x values increase with chain length as with the lamellar phase but the increments are larger. As in the lamellar phase the increment between heptyl and octyl is greater than that between nonyl and decyl.

β-OG shows typical lyotropic liquid crystal property

As noted before, β-OG has successfully been used for crystallizing many membrane proteins, and shows all three lyotropic liquid crystal phases over the wide range of temperature, as summarized in Table IV. A question arising from this connection is whether this elegant lyotropic liquid crystal property of β-OG plays

a role in membrane protein crystallization. At this point, it is very hard to extract a general idea about the role of surfactant molecules in terms of lyotropic liquid crystal properties, because of a lack of information about other surfactants which have been successfully used for crystallizing membrane proteins. However, some speculation about it is meaningful. The outstanding lyotropic liquid crystal property of β-OG may represent higher 'adaptability' against different levels of hydration than that of other related *n*-alkyl pyranosides, and this could be a factor in crystallizing membrane proteins. This higher adaptability will contribute to a balance in the variety of protein-surfactant micelle interactions: a con-

TABLE III

The mean observed spacings, $\langle d_x \rangle$, and the width at half-height intensity, $\Delta\theta^0$, for the micellar solutions of the heptyl to decyl β-glucopyranosides

Surfactants	$\langle d_x \rangle$ (Å)	$\Delta\theta(^0)$ at half height
Heptyl	27.4	0.76
Octyl	33.8	1.03
Nonyl	34.6	0.81
Decyl	37.0	0.93

TABLE IV

Optical and diffraction properties of the lyotropic mesophases of n-alkyl β-D-glucopyranosides

β-D-Glucopyranosides: HG, heptyl; OG, octyl; NG, nonyl; DG, decyl. Phases: L, lamellar; C, cubic; H, hexagonal; M, micellar. Optical and diffraction properties: U, unobserved; A, anisotropic through polarizing microscope; I, isotropic through polarizing microscope; 1L, 1-D lamellar; 3F, 3-D face-centered cubic; 2H, 2-D hexagonal; D, diffuse ring X-ray diffraction pattern.

Phases	HG [a]	OG [b]	NG	DG
L	A, 1L	A, 1L	A, 1L	A, 1L
C	U	I, 3F, D	U	U
H	U	A, 2H	U	U
M	I, D	I, D	I, D	I, D

[a] All three lyotropic liquid crystal phases were observed at 0°C.
[b] All three lyotropic liquid crystal phases were formed over the range of 0°C to room temperature, with slower rate of formation as the temperature decreases.

cept which is often used for describing the role of surfactant molecules in membrane protein crystallization [23,24].

Appendix

The mean thickness of surfactant bilayer in the lamellar phase upon the surfactant concentration is given by

$$\langle d_1 \rangle = \phi \cdot \langle d_x \rangle \tag{A-1}$$

where $\langle d_x \rangle$ is the mean measured X-ray spacing.

In the cubic phase the radius of molecular cluster is given by

$$r_c = [(3 \cdot \bar{a}^3 \cdot \phi)/(4 \cdot \pi \cdot Z)]^{1/3} \tag{A-2}$$

where $\bar{a}$ is the cell dimension and Z is the number of molecular clusters per unit cell which is 4 for Fm3m (face-centered cubic).

In the hexagonal phase the mean radius of the cylinders is given by

$$\langle r_h \rangle = [(\sqrt{3} \cdot \langle \bar{a} \rangle^2 \cdot \phi)/(2 \cdot \pi)]^{1/2} \tag{A-3}$$

where $\langle \bar{a} \rangle$ is the mean periodicity of the two-dimensional P6 lattice.

In these expressions ϕ is the volume concentration of the surfactant given by

$$\phi = [1 + \nu_w (1 - c)/(\nu_s \cdot c)]^{-1}$$

where c is the weight concentration of the surfactant and ν_w and ν_s are the partial specific volumes of the water and surfactant, respectively.

Acknowledgments

References

1 Michel, H. and Oesterhelt, D. (1980) Proc. Natl. Acad. Sci. USA 77, 1283–1285.
2 Garavito, R.M. and Rosenbusch, J.P. (1980) J. Cell Biol. 86, 327–329.
3 Baron, C. and Thomson, T.E. (1975) Biochim. Biophys. Acta 382, 276–285.
4 Stubbs, G.W., Smith, H.G. and Litman, B.J. (1976) Biochim. Biophys. Acta 426, 46–56.
5 Lin, J.T., Riedel, S. and Kinne, R. (1979) Biochim. Biophys. Acta 557, 179–187.
6 Rosevear, P., VanAken, T., Baxter, J. and Ferguson-Miller, S. (1980) Biochemistry 19, 4108–4115.
7 Garavito, R.M., Markovic-Housley, Z. and Jenkins, J.A. (1986) J. Cryst. Growth 76, 701–709.
8 McPherson, A., Koszelak, S., Axelrod, H., Day, J., Williams, R., Robinson, L., McGrath, M. and Cascio, D. (1986) J. Biol. Chem. 261, 1969–1975.
9 Dorset, D.L. and Rosenbusch, J.P. (1981) Chem. Phys. Lipids 29, 299–307.
10 Brown, G.H. and Wolken, J.J. (1979) Liquid Crystals and Biological Structures, pp. 35–42, Academic Press, New York, San Francisco and London.
11 Caffrey, M. (1989) Biophys. J. 55, 47–52.
12 Luzzati, V. (1968) in Biological Membranes (Chapman, D., ed.), pp. 71–123, Academic Press, London and New York.
13 Jeffrey, G.A., Yeon, Y. and Abola, J. (1987) Carbohydr. Res. 169, 1–11.
14 Moews, P.C. and Knox, J.R. (1976) J. Am. Chem. Soc. 98, 6628–6633.
15 Jeffrey, G.A. (1984) Mol. Cryst. Liq. Cryst. 110, 221–237.
16 Jeffrey, G.A. (1986) Acc. Chem. Res. 19, 168–173.
17 Jeffrey, G.A. and Mitra, J. (1983) Acta Cryst. B39, 469–480.
18 Muller-Fahrnow, A., Zabel, V., Steifa, M. and Hilgenfeld, R. (1986) J. Chem. Soc. Chem. Commun. 21, 1573–1544.
19 Jeffrey, G.A. and Maluszynska, H. (1989) Acta Cryst., in press.
20 Zabel, V., Muller-Fahrnow, A., Hilgenfeld, R., Saenger, W., Pfannemuller, B., Enkelmann, V. and Welte, W. (1986) Chem. Phys. Lipids 39, 313–327.
21 Blaurock, A.E. (1982) Biochim. Biophys. Acta 650, 167–207.
22 Grey, G.W. and Goodby, J.W. (1984) Smectic Liquid Crystals, Leonard Hill, Philadelphia.
23 Michel, H. (1983) Trends Biochem. Sci. 8, 56–59.
24 Garavito, R.M. and Jenkins, A. (1985) Crystallography in Molecular Biology, pp. 3–14, Plenum Press, New York and London.